

## Supplementary Figure Legends

### Supplementary Fig. 1. RIP140-deficiency enhances cell proliferation and tumorigenesis.

**a**, RIP140 mRNA level quantified by RT-qPCR after silencing by two different siRNA specific of human RIP140 (n=4 independent experiments).

**b**, The slope of the curves was extracted using xCELLigence RTCA Software from the curves in Fig. 1a and 1b. The slopes of the curves were higher with siRIP140 than with control siRNA.

**c**, MTT assay in MCF7 cells after RIP140 silencing by siRNA #2 (siRIP#2) (n=3 independent experiments).

**d**, Cell proliferation monitored by xCELLigence in MDA-MB-436 after RIP140 silencing by siRNA #2 (siRIP#2) (n=4 independent experiments).

**e**, The slope of the curves was extracted using xCELLigence RTCA Software from Supplementary 1d for MDA-MB-436 and from cell proliferation monitored by xCELLigence in DU145 and RKO after RIP140 silencing by siRNA #2 (siRIP#2) for 7 days.

**f**, RIP140 expression levels quantified by RT-qPCR (left panel; representative experiment; n=) and immunofluorescence (right panel) in the MEFs used in the study. MEF#1 were immortalized by the 3T3 protocol. MEF#2, #3 and #4 were transformed by the infection of SV40/H-RasV12 expressing retrovirus.

- g**, Cell proliferation monitored by xCELLigence in MEF #1 (n=3 independent experiments).
- h**, ATP level in MEF #1 relative to WT (n=3 independent experiments).
- i**, MTT assay in SV40/H-RasV12-transformed RIP140 WT and KO MEF #3 (representative experiment, n=3 independent experiments).
- j**, Number of colonies from soft agar colony assay of MEF #2 (left panel, Student-t-test) and SV40/H-RasV12-transformed MEF #3 (right panel; n=3 independent experiments).
- k**, Tumor growth curve of H-RasV12-MEF #1 xenografted in nude mice (n=6).
- l**, Pictures of xenografted nude mice with MEF #2 from Fig. 1e.
- m**, Human RIP140 mRNA level quantified by RT-qPCR in MEF #1 stably overexpressing a pEGFP plasmid (WT+GFP) and (KO+GFP) or a pEGFP-hRIP140 plasmid (KO+hRIP140). Primers used are specific for the human RIP140 sequence (representative experiment, n=4 independent experiments).
- n**, Relative MTT assay at day 6 of MEF #1 overexpressing GFP or GFP-hRIP140 (n=3 independent experiments).
- o**, Representative pictures of colony soft agar assays of MEF #1 quantified in 1h.

**Supplementary Fig. 2. Inhibiting glycolysis reduces the growth advantage of RIP140-deficient cells.**

Unless otherwise stated, MEF #1 were used.

**a**, Representative pictures of MEF #1 under glucose starvation.

**b**, MTT assay at day 10 represented in Fig. 2a. RIPKO cell proliferation was expressed as relative to that of WT cells for each glucose concentration.

**c**, MTT assay of MEF #3 following glucose deprivation for 4 days and represented as percent of Glucose 4.5g/L for each cell line (n=3 independent experiments).

**d**, Cell proliferation monitored by xCELLigence upon 2DG treatment (2mM) (left panel). The slope of the curves was extracted using xCELLigence RTCA software (right panel) (representative experiment, n=2 independent experiments).

**e**, MTT assay of MEF #3 upon BrP treatment (100 $\mu$ M) (representative experiment, n=3 independent experiments).

**f**, Relative cell index is represented as percent of control after four days of 2DG treatment (5mM)(representative experiments, n=2; Student-t-test).

**g**, Crystal violet staining of MEF #3 after 3 weeks of 2-DG (5mM) treatment and number of colonies expressed as % of WT Control (n=3 independent experiments). This demonstrates that

RIPKO colonies were more numerous than WT colonies and that 2DG treatment abolished the growth of RIPKO colonies.

**Supplementary Fig. 3. RIP140-deficiency enhances glycolysis.**

**a,** Glycolysis represented as relative ECAR normalized to protein quantity in MEF #3 (representative experiment, n=3 independent experiments).

**b,** Glucose consumption (left panel) and lactate production (right panel) were measured by enzymatic determination (Sigma kit) 18h after changing medium. Values were normalized to cell number and time.

**c,** Extracellular acidification rate (ECAR) normalized by protein content in MDA-MB-436 after siRNA silencing of RIP140 (siRIP#2) for 48h (representative experiment, n=3 independent experiments).

**d,** Glycolysis represented as relative ECAR measured by Seahorse Bioscience Flux Analyzer and normalized to protein quantity in colon (RKO) and prostate cancer cell lines (DU145, PC3) after RIP140 silencing by siRNA (siRIP#2)(representative experiment, n=2 independent experiments).

**Supplementary Fig. 4. GLUT3 and G6PD are essential for the growth advantage induced by RIP140-deficiency.**

**a**, Heatmap of glycolytic genes showing differential expression in MEF #1 obtained from RT-qPCR of two independent samples. Data are expressed as relative to WT (# means at least 2-fold induction).

**b**, *GLUT3* and *G6PD* mRNA levels quantified by RT-qPCR in MEF #3 (n=3 independent experiments).

**c**, mRNA level of *RIP140*, *GLUT3* and *G6PD* quantified by RT-qPCR in MDA-MB-436 (left panel) and MCF7 (right panel) after RIP140 silencing (n=3 independent experiments).

**d**, Quantification with Image J software of western blot analyses shown in Fig. 4b.

**e**, Relative NADPH/NADP<sup>+</sup> ratio quantified in MEF #1 using NADP/NADPH-Glo™ Assay (Promega) (representative experiment, n=3 independent experiments).

**f**, MTT assay of MEF #3 upon 6AN treatment (10μM) (representative experiment, n=3 independent experiments).

**g**, Crystal violet staining of soft agar colonies of MEF #3 after 3 weeks of 6AN (10μM) treatment quantified in Fig. 4f (representative experiment, n=3 independent experiments).

**h**, Cell viability assessed by crystal violet staining of MDA-MB-436 after RIP140 silencing by siRNA at day 7 and represented as percent of control after 6AN (10 $\mu$ M) treatment (n=2 independent experiments).

**i, j**, Knockdown efficiency by specific shRNA of GLUT3 (**i**) or G6PD (**j**) was determined by western blot (left and middle panels) and RT-qPCR (right panel: n=3 independent experiments).

**k**, siRNA efficiency was verified by RT-qPCR for *RIP140*, *GLUT3* and *G6DP* 48h after transfection in MDA-MD-436 used in Fig. 4h.

**l**, Crystal violet staining of soft agar colonies of transformed MEF #1 stably expressing shGLUT3 or shG6PD; quantification of Fig. 4g.

**m**, Cell proliferation measured by MTT assay of MEF #1 stably expressing shGLUT3 or shG6PD (representative experiment, Student-t-Test).

**Supplementary Fig. 5. RIP140 and p53 interact to inhibit the expression of GLUT3.**

**a**, Transient transfection in MDA-MB-436 co-transfected with a G6PD-Luc reporter gene in presence of increasing concentrations of a siRNA specific of RIP140 (siRIP#2) (n=3 independent experiments).

**b**, Transient transfection in MEF #4 co-transfected with GLUT3-Luc or G6PD-Luc reporter genes (n=3 independent experiments).

**c**, Transient transfection in MEF #1 co-transfected with a G6PD-Luc reporter gene in presence of increasing concentrations of a RIP140-expressing plasmid (representative experiment, n=5 independent experiments).

**d**, p53 protein level quantified by western blot in MEF #2 (left panel) and mRNA level quantified by RT-qPCR in MEF #2 and #3 (right panel: n=5 independent experiments for MEF #3).

**e**, p53 mRNA level quantified by RT-qPCR in MEF #1 overexpressing GFP or GFP-hRIP140.

**f**, p53 mRNA level quantified by RT-qPCR in MCF7 after RIP140 silencing (siRIP#2)(n=3 independent experiments).

**Supplementary Fig. 6. RIP140 and p53 inhibit the expression of GLUT3 induced by HIF-**

**2a.**

**a**, Transient transfection in MEF #1 RIPKO co-transfected with a HRE-Luc and increasing concentrations of plasmids expressing HIF-1 $\alpha$  or HIF-2 $\alpha$  in the presence of a RIP140-expressing plasmid (representative experiment, n=3 independent experiments).

**b**, Human HIF mRNA level quantified by RT-qPCR in MEF#1 after transient transfection of the corresponding plasmids (representative experiment, n=3 independent experiments).

**c**, Transient transfection in MEF #1 co-transfected with a GLUT3-Luc reporter gene and increasing concentrations of plasmids expressing HIF-1 $\alpha$  or HIF-2 $\alpha$  (representative experiment, n=3 independent experiments).

**d**, HIF protein level quantified by western blot in MEF #1 in normoxia. Unprocessed original scans of blots are shown in Supplementary Figure 7.

**e**, HIF mRNA level quantified by RT-qPCR in MEF #1 and MEF #4 (n=3 independent experiments).

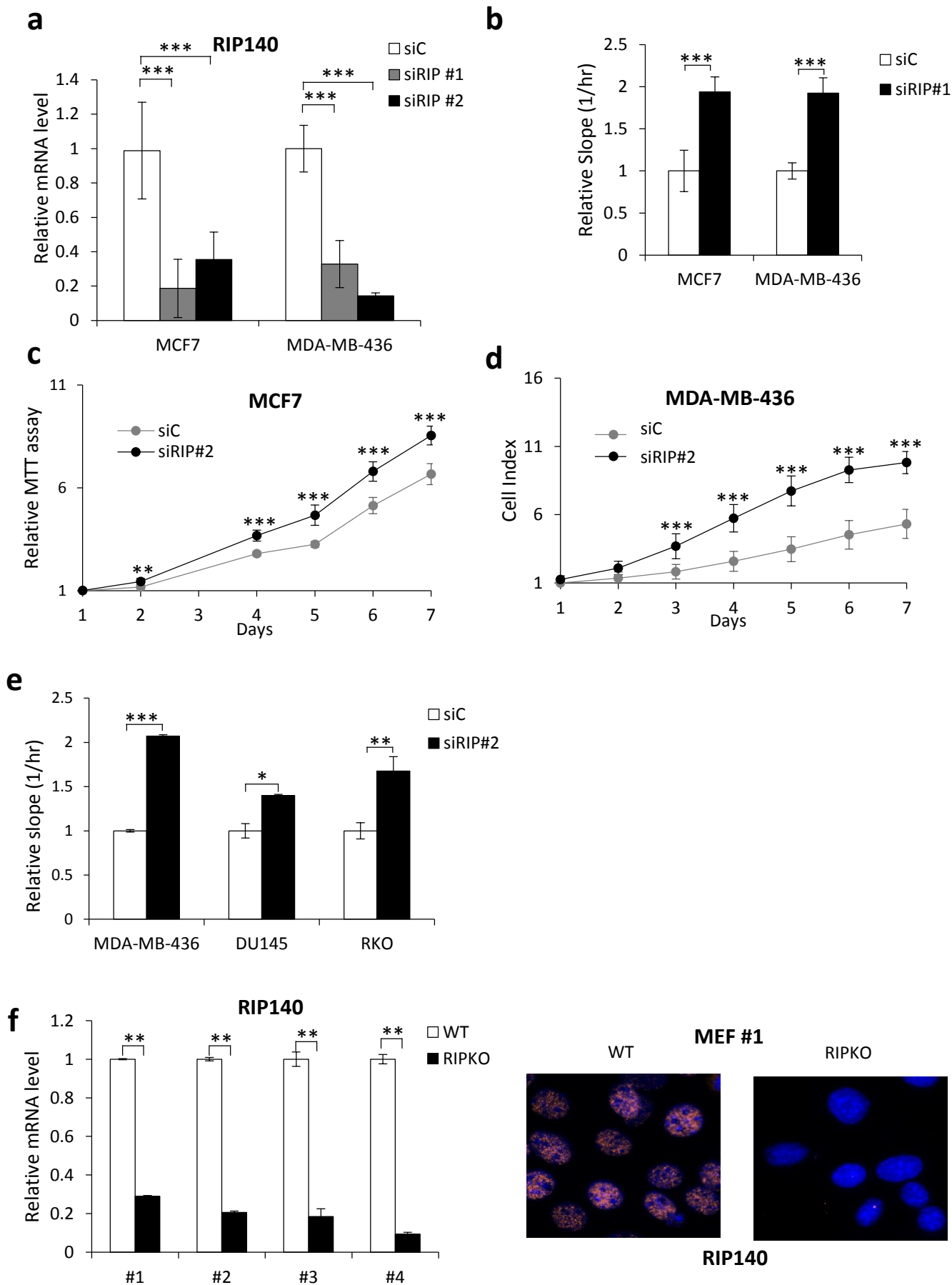
**f**, HIF-2 $\alpha$  mRNA level quantified by RT-qPCR in MEF #1 after siRNA silencing (n=3 independent experiments).

**g**, Proximity ligation assay in MEF p53 null between RIP140 and HIF-2 $\alpha$  using rabbit anti-RIP140 and mouse anti-HIF-2 $\alpha$  and between p53 and HIF-2 $\alpha$  using rabbit anti-HIF-2 $\alpha$  and mouse anti-p53. Right panel: Dots were quantified with the Duolink Software from 5 independent microscopic fields.

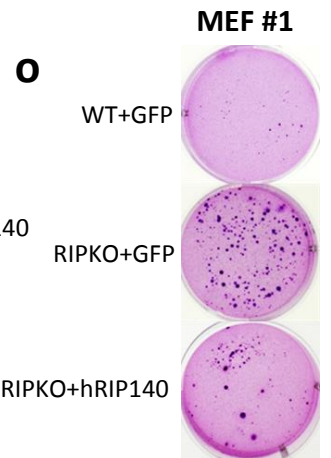
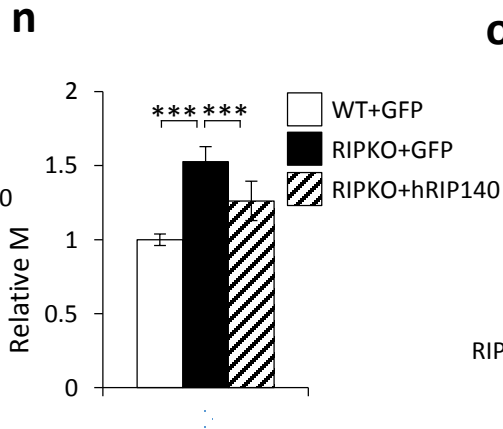
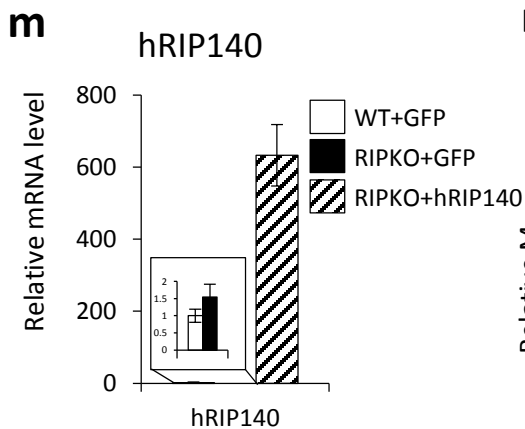
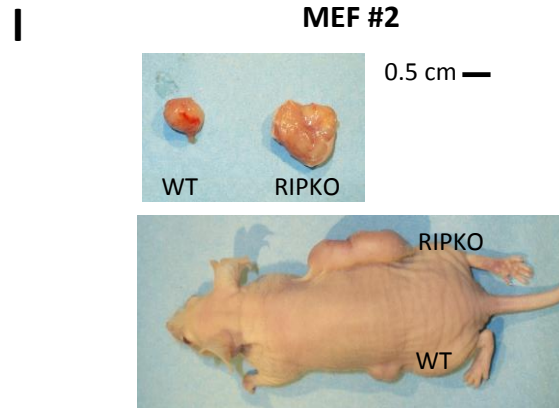
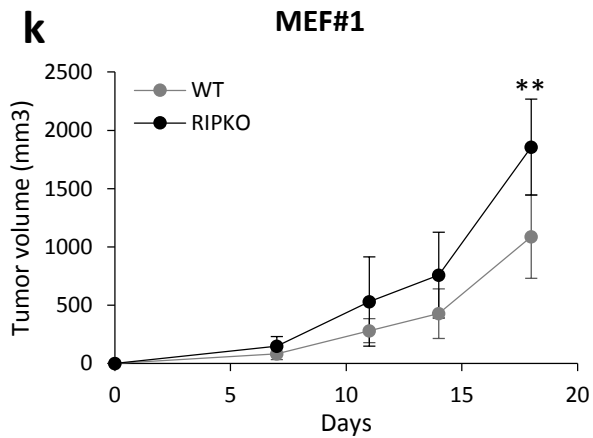
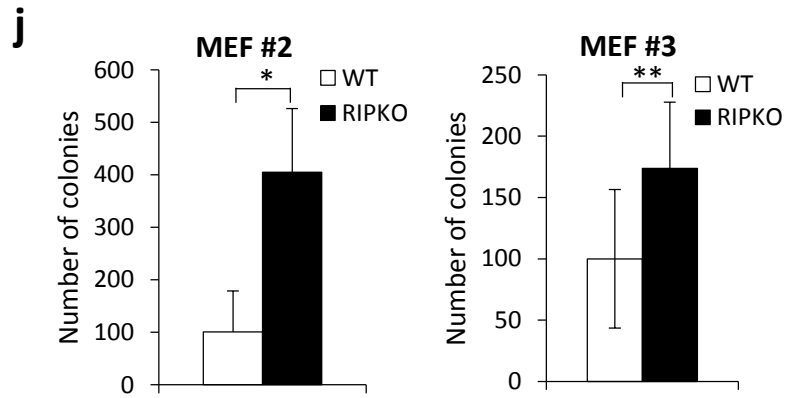
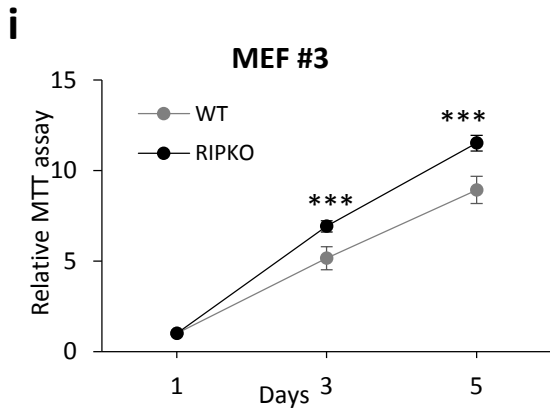
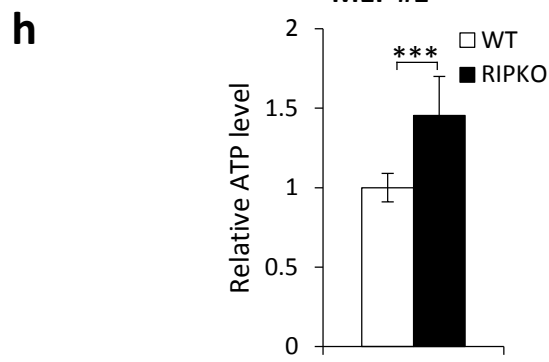
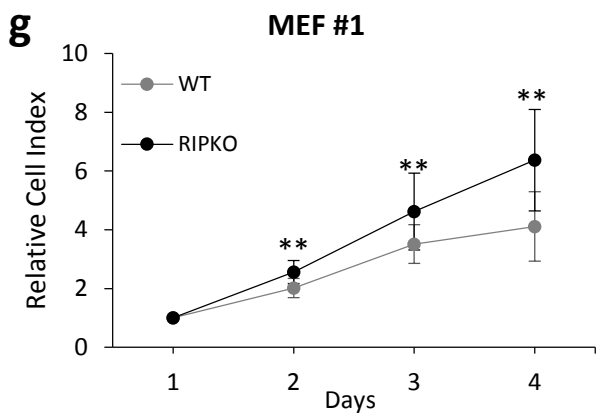
**Supplementary Fig. 7. Unprocessed original scans of blots.**



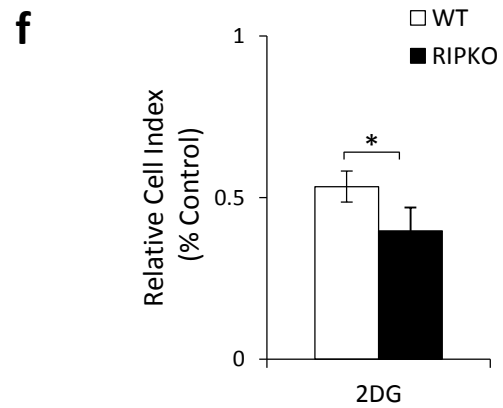
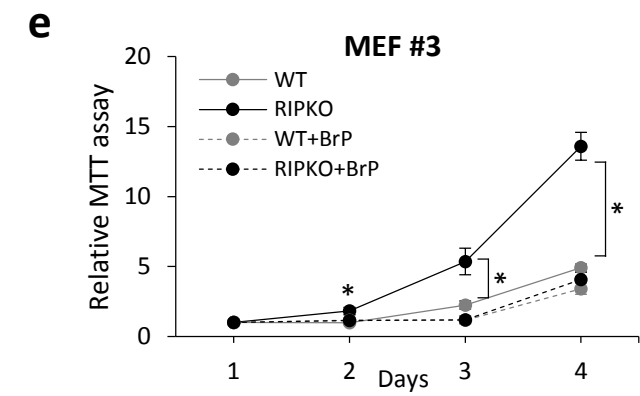
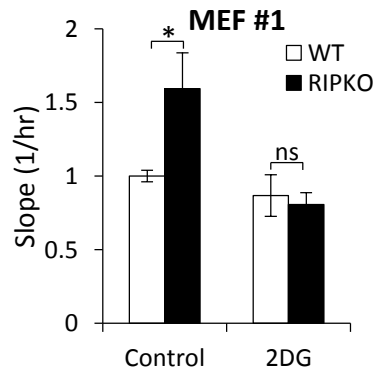
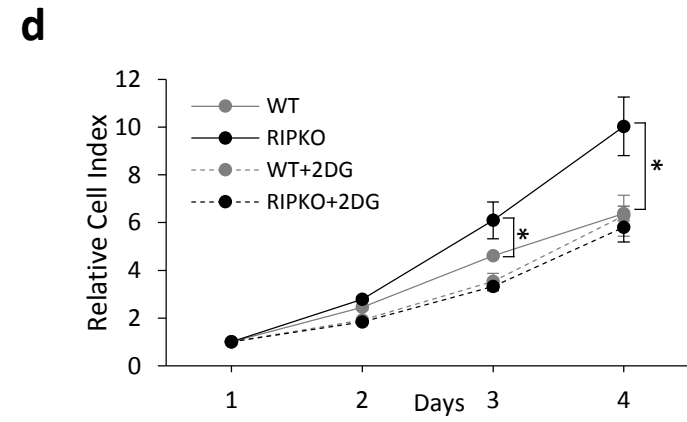
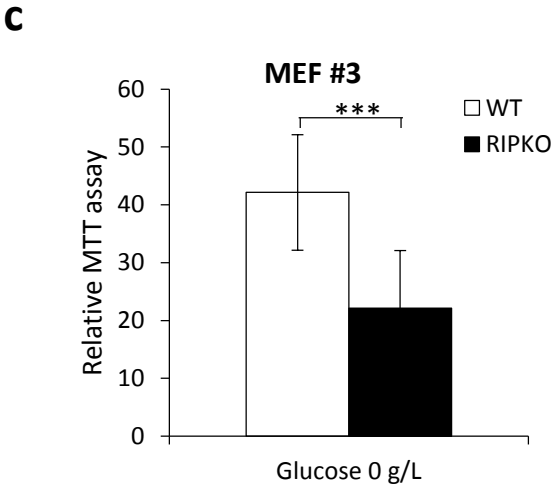
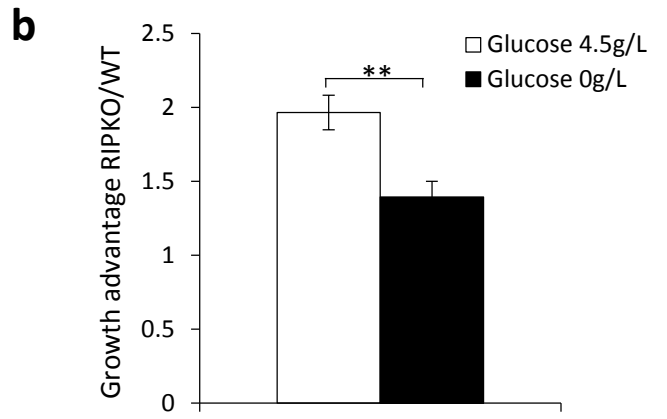
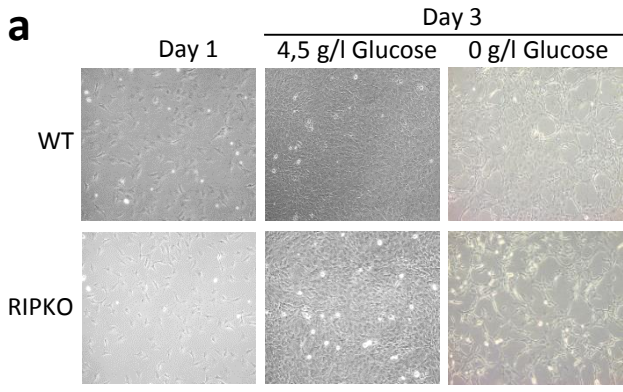
Unprocessed images of all Western blots as indicated. Molecular size markers in kDa.



Supplementary Figure 1.

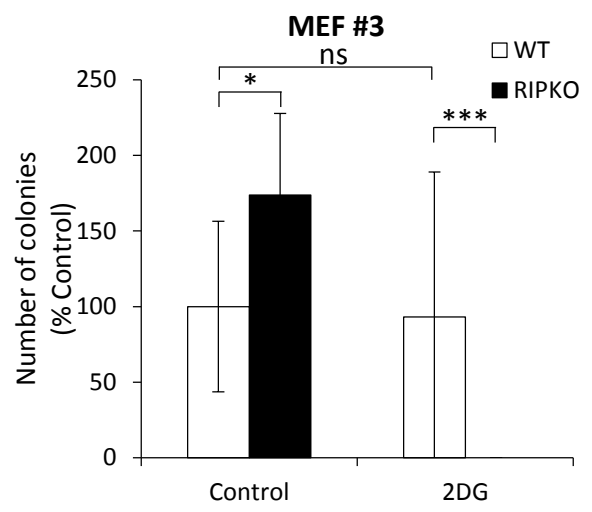
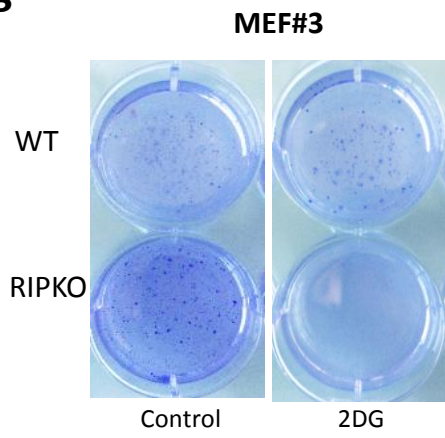


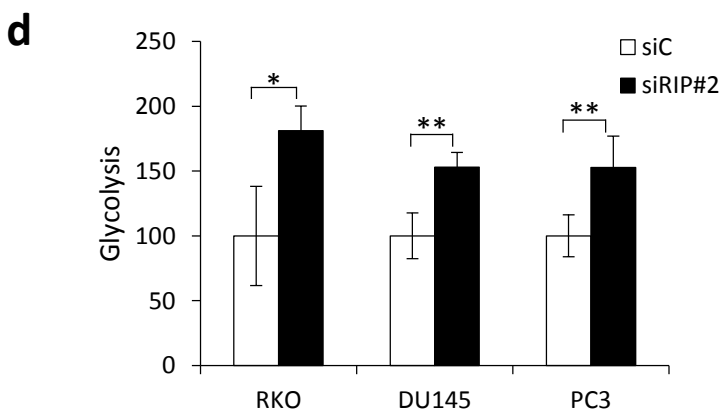
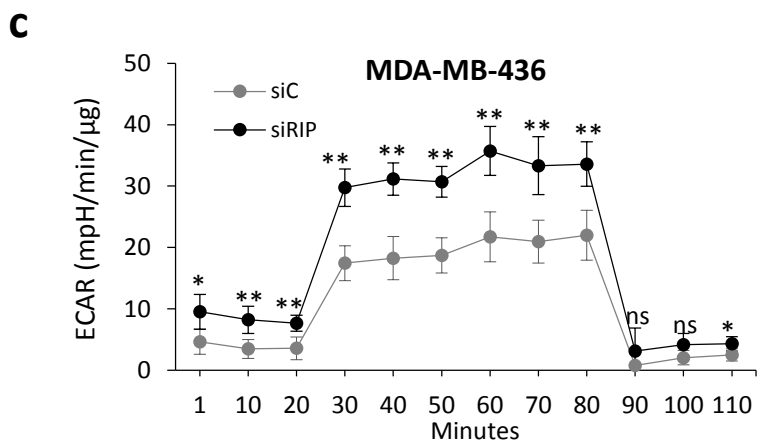
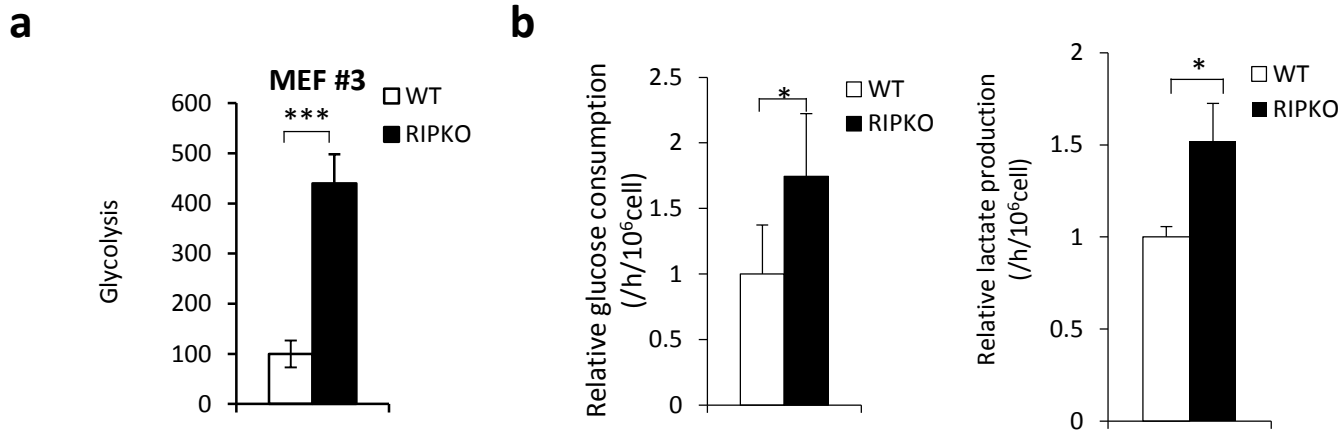
Supplementary Figure 1

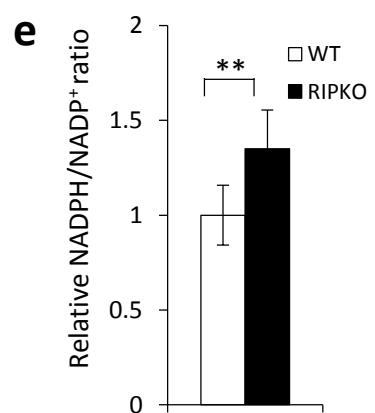
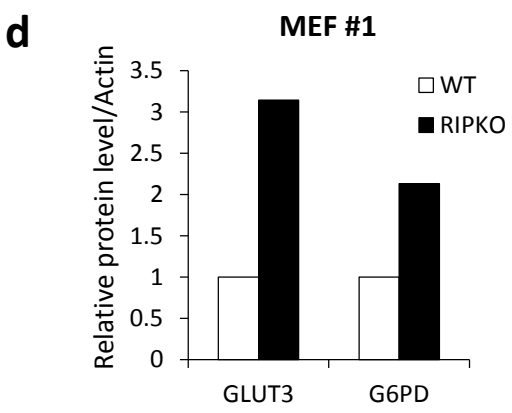
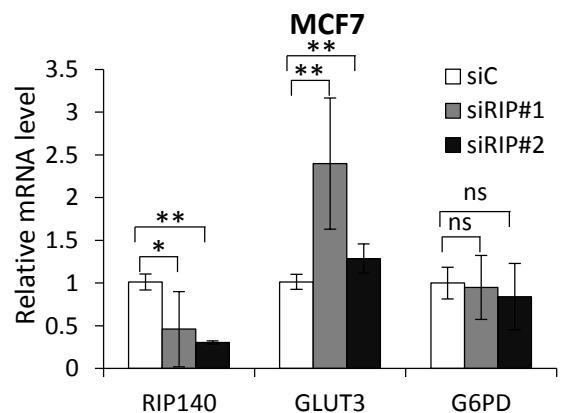
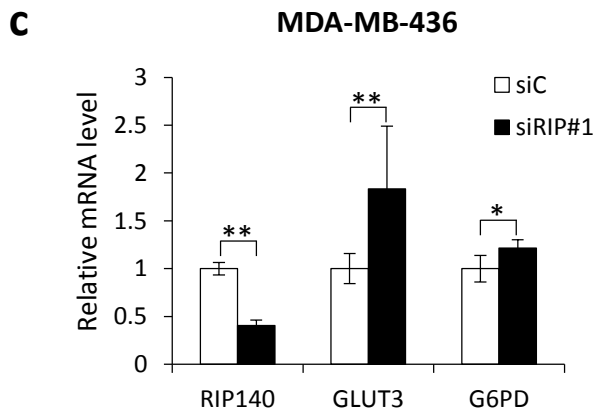
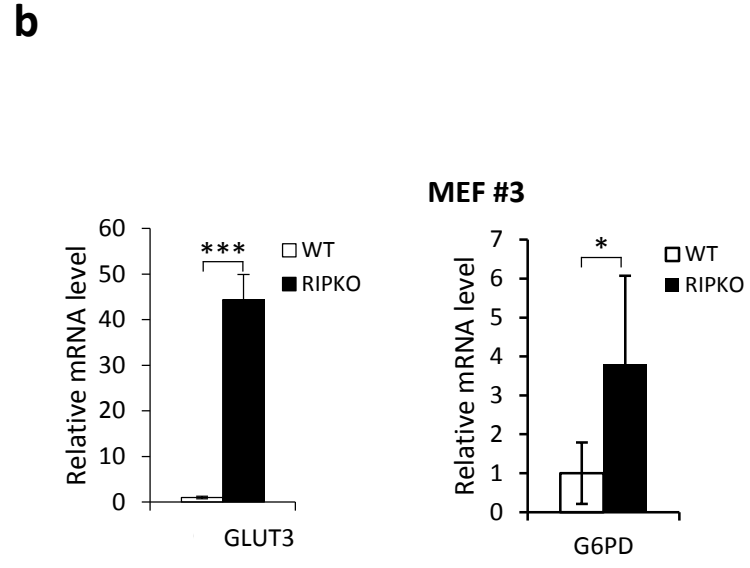
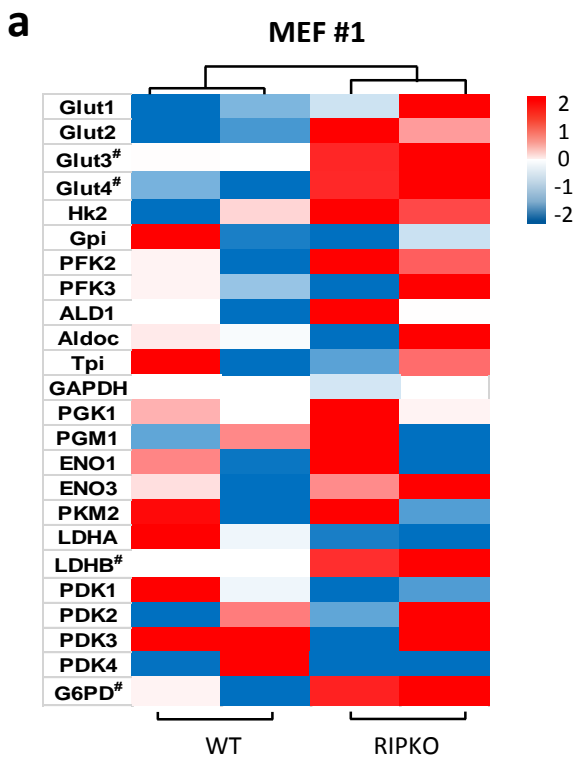


Supplementary Figure 2.

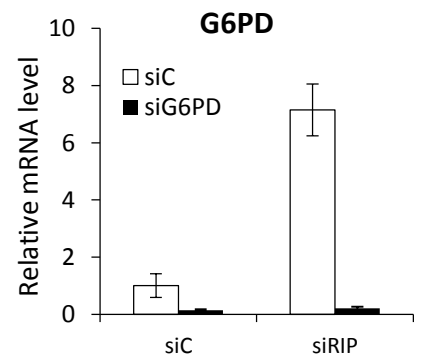
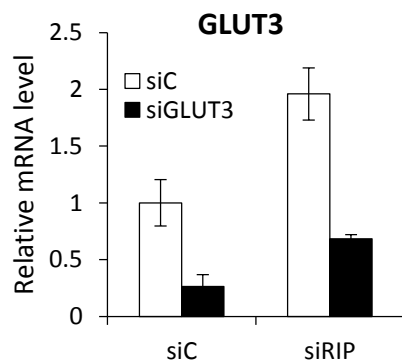
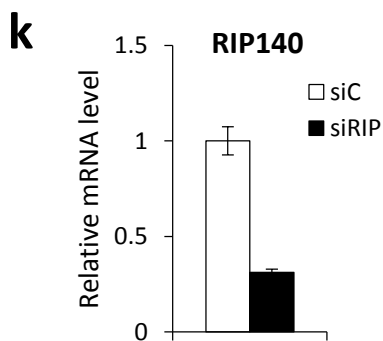
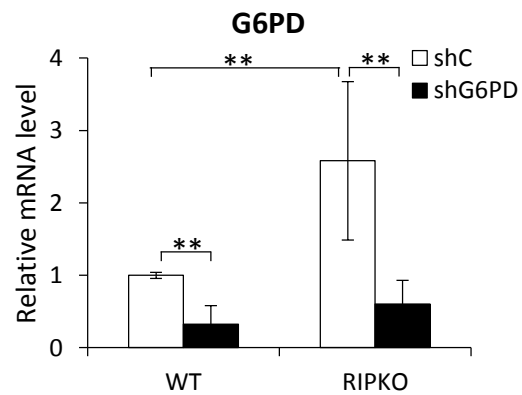
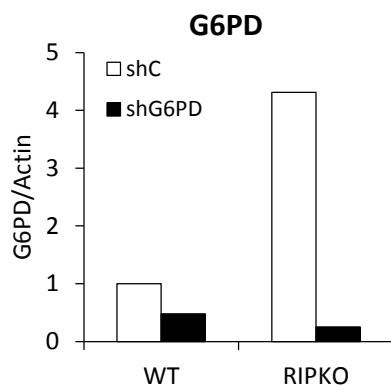
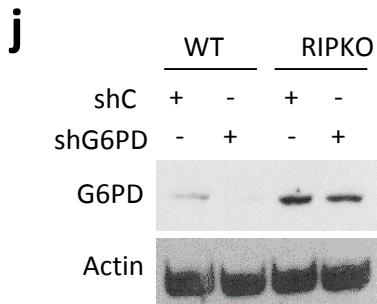
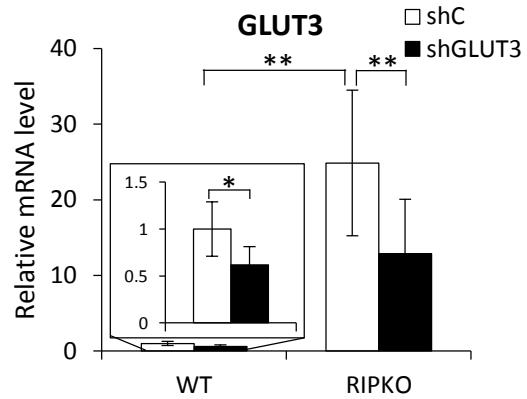
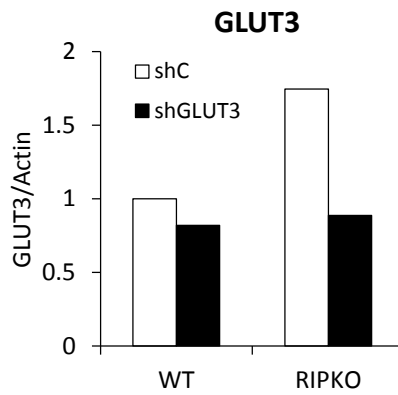
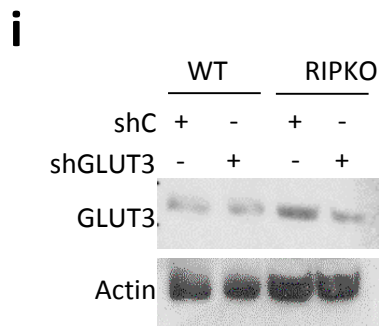
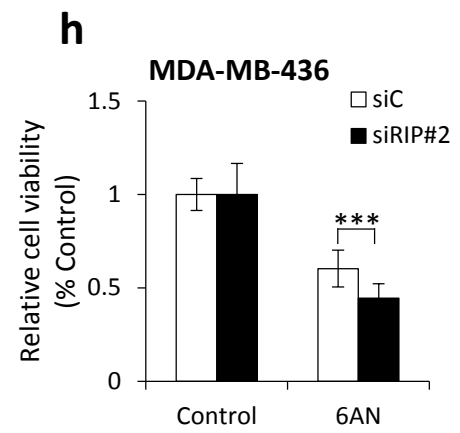
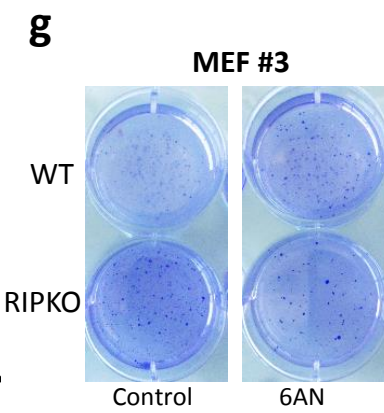
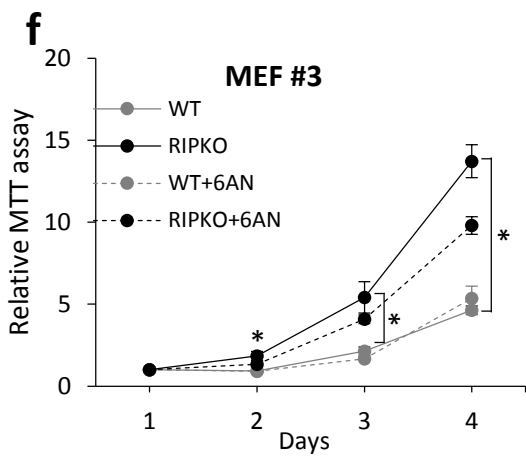
**g**



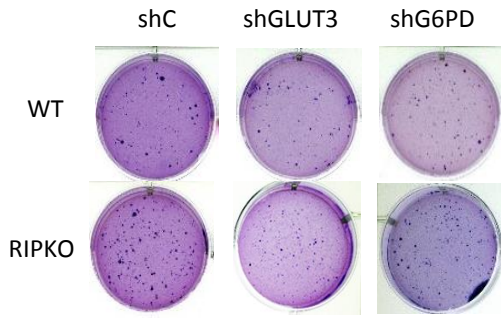
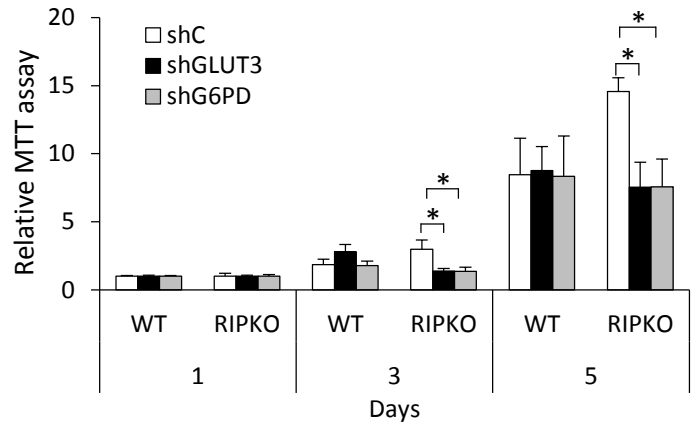


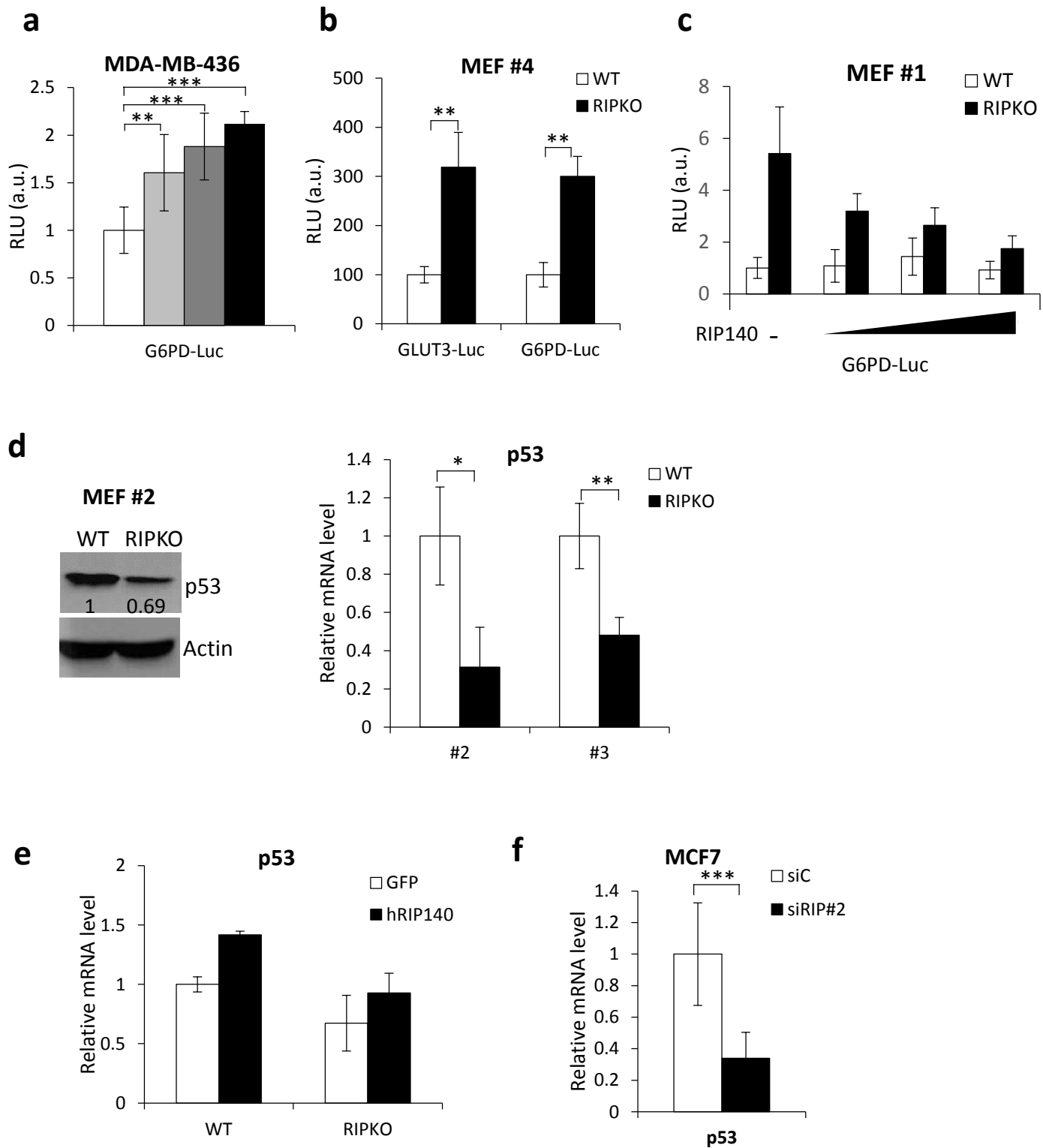


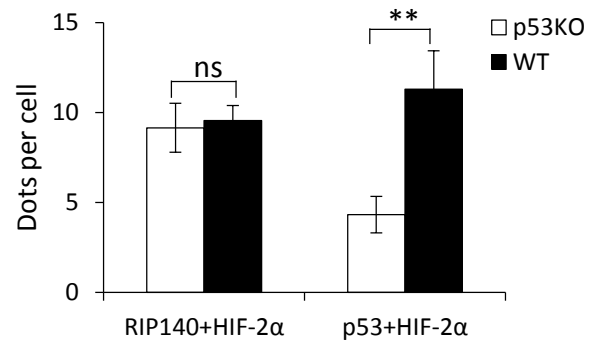
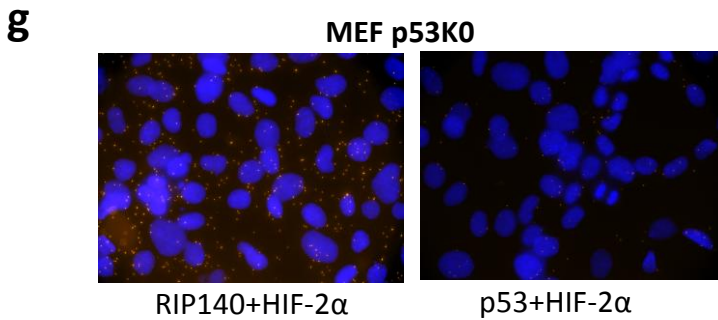
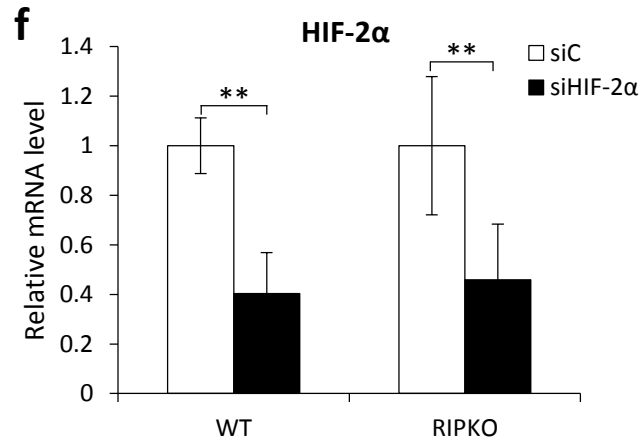
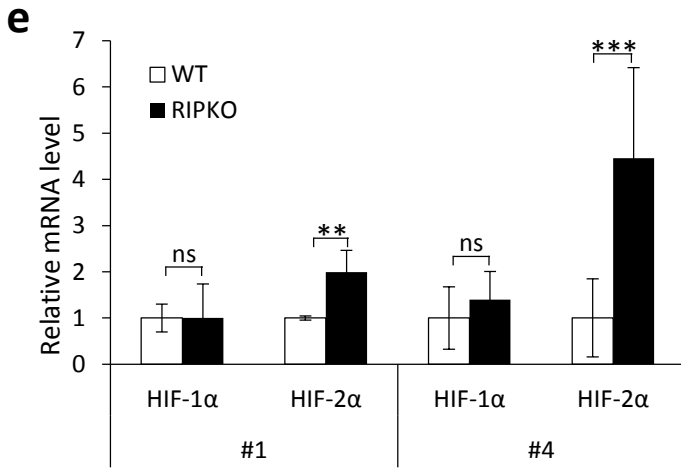
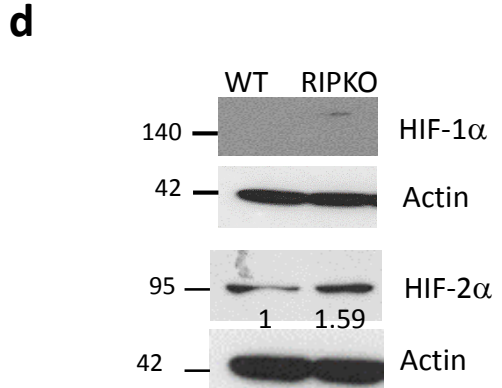
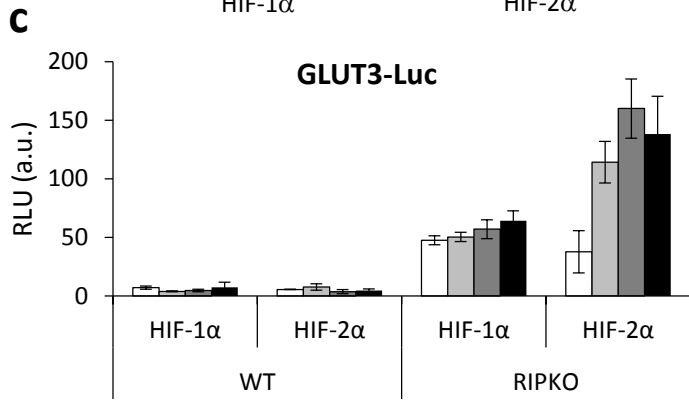
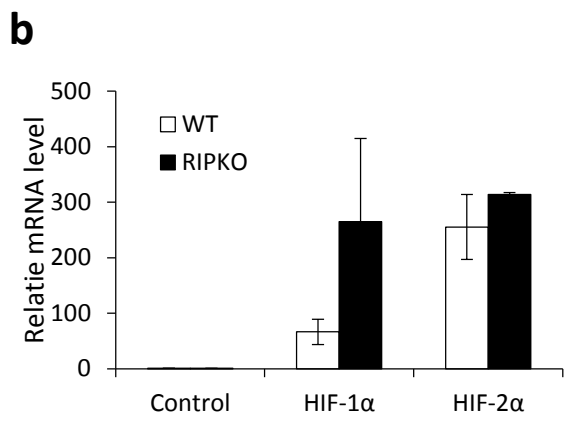
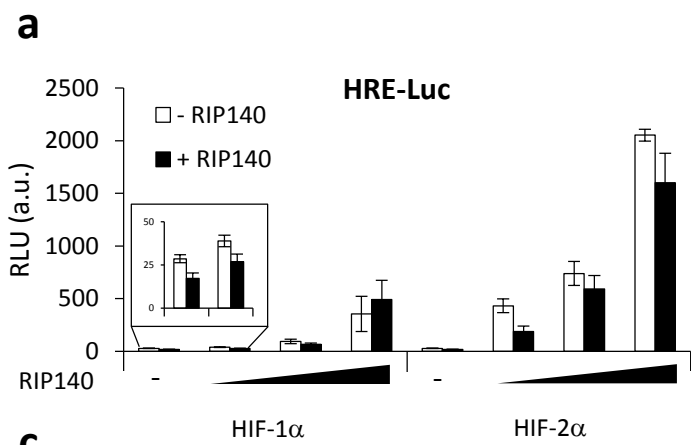
Supplementary Figure 4



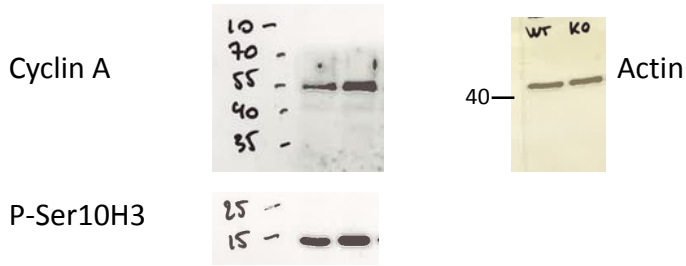


**l****m**

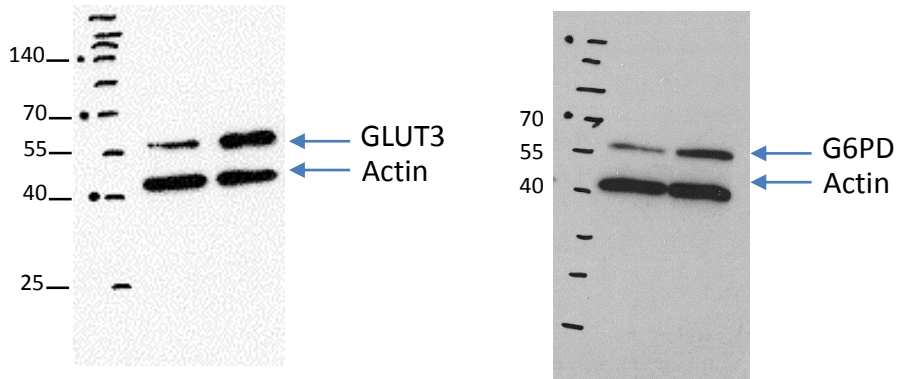




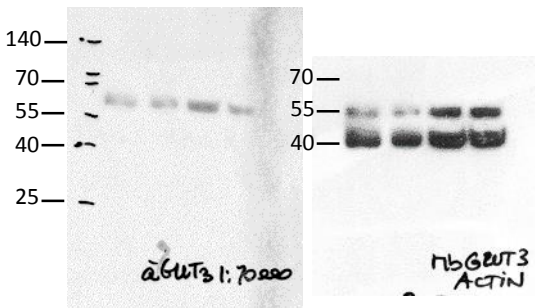
Related to Fig. 1d



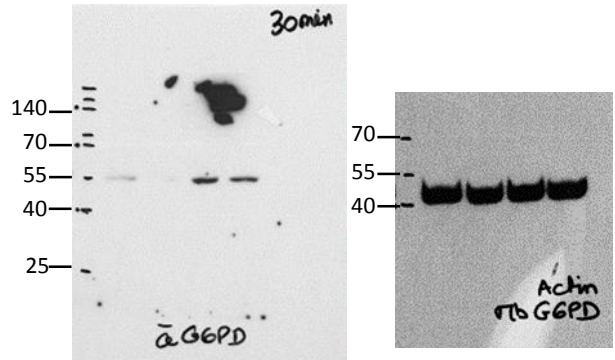
Related to Fig. 4b



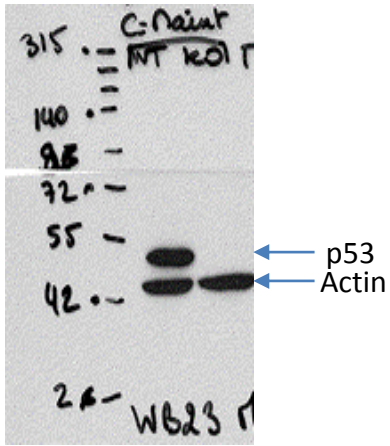
Related to Supplementary Fig. 4i



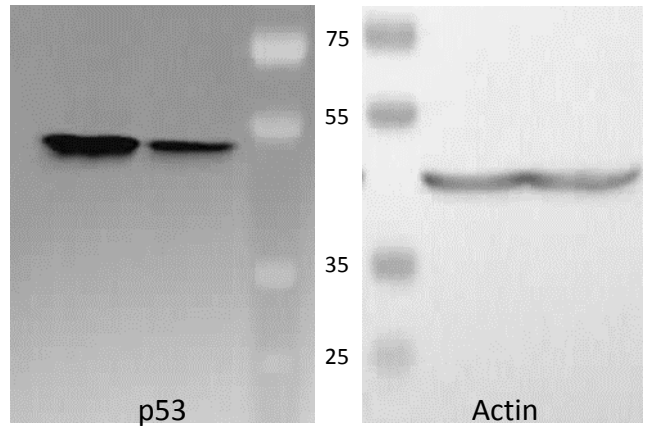
Related to Supplementary Fig. 4j



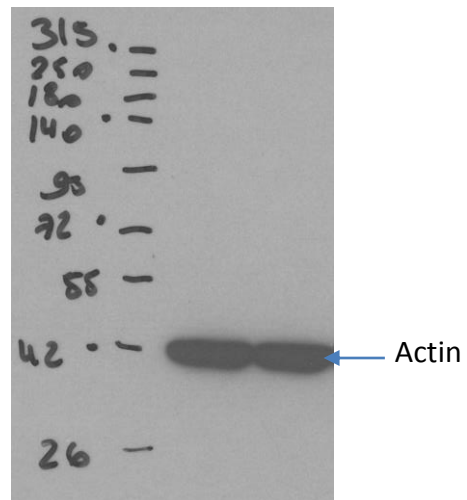
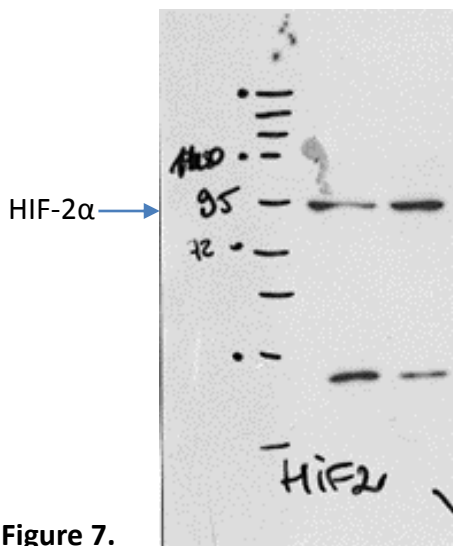
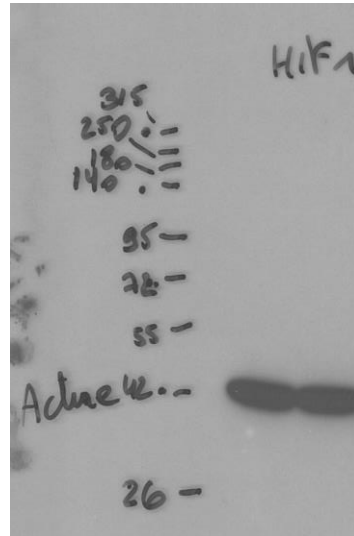
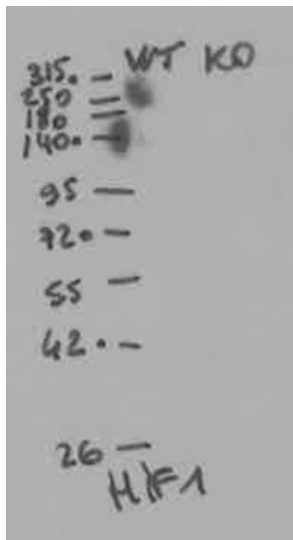
Related to Fig. 5h



Related to Supplementary Fig. 5d



Related to Supplementary Fig. 6d



Supplementary Figure 7.